DRAFT VERSION SEPTEMBER 10, 2012
Preprint typeset using LaTeX style emulateapj v. 5/2/11

CONSTRAINTS ON THE IONIZING EFFICIENCY OF THE FIRST GALAXIES

MARCELO A. ALVAREZ[1], KRISTIAN FINLATOR[2] AND MICHELE TRENTI[3]

Draft version September 10, 2012

ABSTRACT

Observations of the Lyman-α forest and of high-redshift galaxies at $z \sim 6-10$ imply that there were just enough photons to maintain the universe in an ionized state at $z \sim 5-6$, indicating a "photon-starved" end to reionization. The ionizing emissivity must have been larger at earlier times in order to yield the extended reionization history implied by the electron scattering optical depth constraint from WMAP. Here we address the possibility that a faint population of galaxies with host halo masses of $\sim 10^{8-9} M_{\odot}$ dominated the ionizing photon budget at redshifts $z \gtrsim 9$, due to their much higher escape fractions. Such faint, early galaxies, would not have formed in ionized regions due to suppression by heating from the UV background, and would therefore not contribute to the ionizing background at $z \lesssim 6$, after reionization is complete. Our model matches: (1) the low escape fractions observed for high-redshift galaxies, (2) the WMAP constraint of $\tau_{\rm es} \sim 0.09$, (3) the low values for the UVB at $z < 6$, and (4) the observed star formation rate density inferred from Lyman-break galaxies. A top heavy IMF from Pop III stars is not required in this scenario. We compare our model to recent ones in the literature that were forced to introduce an escape fraction that increases strongly towards high redshift, and show that a similar evolution occurs naturally if low mass galaxies possess high escape fractions.

Subject headings: cosmology: theory — dark ages, reionization, first stars — intergalactic medium

1. INTRODUCTION

A fundamental question in the theory of reionization is: *what were the ionizing sources?* While it was realized several decades ago that the observed quasar population was insufficient (Shapiro & Giroux 1987), the actual sources have eluded detection. The main constraints on reionization models are the Gunn-Peterson trough (Gunn & Peterson 1965) in the spectra of high redshift quasars at a redshift of $z \sim 6$ (e.g., Fan et al. 2002; Willott 2007), and the electron scattering optical depth, $\tau_{\rm es}$, with the latest results indicating that the universe was substantially ionized by $z \sim 10$ (Komatsu et al. 2011). Models adhering to these constraints predict extended reionization histories (e.g., Haiman & Holder 2003; Cen 2003; Wyithe & Loeb 2003; Ricotti & Ostriker 2004; Choudhury & Ferrara 2006; Fan et al. 2006; Haiman & Bryan 2006; Iliev et al. 2007; Kuhlen & Faucher-Giguère 2012; Haardt & Madau 2012; Ahn et al. 2012).

The ionizing emissivity observed at $z \sim$4–6 is too low to account for the observed $\tau_{\rm es}$. Bolton & Haehnelt (2007) found that extrpolating the ionizing emissivity inferred from the Lyman-α forest at $z \sim$4–6 to higher redshifts would underproduce $\tau_{\rm es}$. Likewise, observations of "Lyman-break galaxies" (LBGs) at $z > 6$ indicate a rapidly declining star formation rate in the brightest galaxies toward high redshift (Oesch et al. 2012), consistent with evolution of the dark-matter halo mass function (Trenti et al. 2010). The ionizing emissivity from these galaxies can reionize the universe by $z \sim 6$, under fairly generous assumptions regarding uncertainties such as the ionizing escape fraction, the intergalactic medium temperature, and the abundance of galaxies fainter than the current detection limit (Trenti et al. 2010; Bouwens et al. 2011). Thus, both observations of the high-redshift galaxy population *and* of the Lyman-α forest indicate a photon-starved end to reionization.

Reconciling the ionizing emissivity observed at $z \sim 4-6$ with the $\tau_{\rm es}$ value has been the subject of recent work. Kuhlen & Faucher-Giguère (2012) presented a model that matches both a photon-starved end to reionization and the WMAP result. In their best-fitting model, the escape fraction, $f_{\rm esc}$, varies with redshift, while the relation between halo mass and ionizing luminosity is extrapolated from abundance matching at lower redshift. The "minimal reionization model" adopted by Haardt & Madau (2012, – HM12 hereafter) also assumes $f_{\rm esc}$ increases with redshift. Fontanot et al. (2012) find that either an increasing $f_{\rm esc}$ towards high redshift and/or towards fainter galaxies is required. Shull et al. (2012) argue instead for an end of reionization of $z \approx 7$ and a $\tau_{\rm es}$ at the low-end of the WMAP allowed range.

Here we investigate the scenario in which low mass galaxies have a much higher $f_{\rm esc}$ than more massive ones, but do not survive past reionizion. We separate halos into two categories based on their mass. Low-mass halos are subject to complete suppression by a photoionizing background and are called "photosuppressible", while more massive halos are not sensitive to an ionizing background. Under these circumstances, photosuppression effects naturally extend the reionization process (e.g., Haiman & Holder 2003; Wyithe & Loeb 2003; Choudhury & Ferrara 2006; Iliev et al. 2007). We further assume that low-mass halos have similar star formation efficiencies to their high-mass counterparts, but have much higher escape fractions, of order unity. Before proceeding, we first discuss the two main physical motivations for our model.

First, theoretical models and observations indicate the ionizing photon $f_{\rm esc}$ should vary with halo mass. Star formation in the lowest-mass galaxies was likely bursty, taking place in a highly irregular gas distributions more resembling massive star forming regions than rotationally supported disks. As illustrated by the numerical simulations pre-

malvarez@cita.utoronto.ca
[1] Canadian Institute for Theoretical Astrophysics, University of Toronto, 60 St.George St., Toronto, ON M5S 3H8, Canada
[2] Department of Physics, University of California Santa Barbara, Santa Barbara, CA 93106, USA
[3] Institute of Astronomy, University of Cambridge, Madingley Road, Cambridge, CB3 0HA, United Kingdom

sented by Wise & Cen (2009), stars should be able to carve out channels through which radiation can escape. For higher mass halos, the escape fraction should only reach a few per cent, because most of the ionizing radiation is produced deep within the galaxy's disk and absorbed (Gnedin et al. 2008; Razoumov & Sommer-Larsen 2010). In support of this picture, observations at $z \sim 3$ indicate that Lyman Break galaxies possess low ionizing escape fractions ($< 10\%$; Shapley et al. 2006; Siana et al. 2010) while fainter galaxies show escape fractions that grow comparable to unity (Iwata et al. 2009; Nestor et al. 2011).

Second, photoionization heating has a negative feedback effect on star formation in dwarf galaxies (Efstathiou 1992). Shapiro et al. (1994) investigated the linear growth of gas perturbations, finding a filtering scale that lags behind the instantaneous Jeans scale, and Gnedin & Hui (1998) presented convenient analytical formulae for the filtering scale. Subsequent coupled radiation-hydrodynamical simulations confirmed the negative feedback effect of photoionization heating (Thoul & Weinberg 1996; Gnedin 2000; Dijkstra et al. 2004; Okamoto et al. 2008). The latest simulations by Finlator et al. (2011) indicate a suppression scale of a few times 10^9 $M_\odot$. Photoionization heating will have a significant negative effect on star formation in the faintest, most abundant, early galaxies.

In this paper we attempt to find the simplest possible reionization model that satisfies current constraints. An important simplifying assumption we have made is the same halo mass threshold for the escape fraction *and* photosuppression – in our fiducial model, halos with masses below $2 \times 10^9 M_\odot$ have both high escape fractions and are subject to photosuppression. A common mass scale is physically plausible, however, given that it is the same mechanism (photoionization feedback) which is likely to be responsible both for higher escape fractions and suppression in low-mass halos.

We present our model in §2, results in §3, and a discussion in §4. All distances and densities are in comoving units, and we adopt cosmological parameters consistent with the latest WMAP constraints (Komatsu et al. 2011), $(\Omega_m, \Omega_\Lambda, \Omega_b, h, \sigma_8, n_s) = (0.275, 0.725, 0.046, 0.7, 0.82, 0.97)$.

2. MODEL

We obtain the hydrogen ionized fraction, $x(z)$, using the following relationship (e.g., Shapiro & Giroux 1987; Haardt & Madau 2012):

$$\dot{x} = \frac{\dot{n}_\gamma}{n_0} - \frac{x}{\langle t_{\rm rec} \rangle}, \quad (1)$$

where $\dot{n}_\gamma$ is the comoving ionizing photon emissivity, $n_0 = n_{\rm H} + n_{\rm He}$ is the comoving number density of hydrogen and helium nuclei, and the recombination time is $\langle t_{\rm rec} \rangle^{-1} = n_0 \alpha_B c_l(z)(1+z)^3$. We use the clumping factor $c_l = C_{100}$ obtained by Pawlik et al. (2009) for their $z_{\rm reion} \sim 10.5$ case, $c_l = e^{-0.28z+3.59} + 1$ for $z > 10$ and $c_l = 3.2$ for $z < 10$, consistent with the transmissivity and mean free path reported in the literature (Songaila & Cowie 2010; Kuhlen & Faucher-Giguère 2012). Helium is singly ionized along with hydrogen, with He II reionization occurring later, at $z = 3$.

The ionizing emissivity is related to the star formation rate density (SFRD) via

$$\dot{n}_\gamma = f_{\rm esc,1} f_\gamma \dot{\rho}_{*,1} + f_{\rm esc,2} f_\gamma \dot{\rho}_{*,2} \quad (2)$$

where $f_{\rm esc,i}$ corresponds to type i halos, f_γ is the number of ionizing photons produced per stellar mass formed, and $\dot{\rho}_{*,i}$ is the SFRD of type i halos. Type 1 (photosuppressible) halos can only host sources of ionizing radiation if they are in neutral regions, while more massive type 2 halos can host sources even after reionization.

We use a Salpeter IMF, with $M_{\rm min} = 0.1 M_\odot$, $M_{\rm max} = 100 M_\odot$. At solar metallicity with this IMF, $f_\gamma \simeq 3 \times 10^{60} M_\odot^{-1}$ (e.g., Haardt & Madau 2012, and references therein), while for a metal poor population with $Z = 0.02 Z_\odot$, $f_\gamma \simeq 5 \times 10^{60} M_\odot^{-1}$, and for the $Z = 0$ case $f_\gamma \simeq 7 \times 10^{60} M_\odot^{-1}$ (Schaerer 2002). We assume that the ionizing photons are emitted instantaneously, which is an excellent approximation given the lifetime of the massive stars that produce the bulk of the ionizing radiation.

The SFRD is given by

$$\dot{\rho}_* = \dot{\rho}_{*,1} + \dot{\rho}_{*,2} = \rho_0 \frac{\Omega_b}{\Omega_m} \left[(1-x) \epsilon_{*,1} \dot{f}_1 + \epsilon_{*,2} \dot{f}_2 \right], \quad (3)$$

where $\epsilon_{*,i}$ is the fraction of baryons converted to stars in halos in the mass range i with collapsed fraction f_i. The $(1-x)$ factor in the first term accounts for the suppression of star formation in ionized regions for photosuppressible halos. We will use M_1 and M_2 to indicate the lower mass limits of our two halo mass ranges. Equations (1), (2), and (3) are solved simultaneously to obtain the ionized fraction, ionizing emissivity, and star formation rate density as a function of redshift.

The electron scattering optical depth from reionization is

$$\tau_{\rm es} = \frac{3 H_0 \Omega_b c \sigma_T}{8 \pi G m_p} \int_0^\infty \frac{x(z)(1+z)^2 (1 - Y + N_{He}(z) Y/4)}{\sqrt{\Omega_m (1+z)^3 + 1 - \Omega_m}} dz, \quad (4)$$

where $Y \simeq 0.24$ is the helium abundance and $N_{\rm He}(z)$ is the number of times helium is ionized – we use $N_{\rm He} = 2$ for $z < 3$ and $N_{\rm He} = 1$ for $z > 3$.

3. RESULTS

Shown in Figure 1 are our results for our three models. The first two, "suppression" and "no suppression", were obtained using the model in §2. In both cases, $M_1 = 10^8 M_\odot$ (roughly the mass at which atomic cooling is efficient), $M_2 = 2 \times 10^9 M_\odot$ (the mass at above which star formation can proceed in ionized regions), $f_{\rm esc,2} = 0.05$, and $\epsilon_{*,1} = \epsilon_{*,2} = 0.03$. In the no suppression model, we removed the $1-x$ factor on the right hand side of equation (3). We restricted $\epsilon_{*,1} \leq \epsilon_{*,2}$, since internal feedback effects are stronger at lower masses, and $\epsilon_{*,2} = 0.03$ was chosen so as to match the overall efficiency found of halos with $M > 2 \times 10^9 M_\odot$ in the Trenti et al. (2010) ICLF model (see Figure 1 and discussion below). We chose $f_{\rm esc,2} = 0.05$ to be consistent with the relatively low escape fractions inferred for observed LBGs. We varied the remaining parameter, $f_{\rm esc,1}$, in both cases to obtain $\tau_{\rm es} = 0.086$, so that $f_{\rm esc,1} = 0.8$ and $f_{\rm esc,1} = 0.45$ in the cases with and without suppression, respectively.

The last model shown is our implementation of the "minimal reionization" model of HM12, with a constant value of f_γ. In their implementation, the metallicity is assumed to follow $Z(z) = Z_\odot 10^{-0.15z}$, which corresponds to a value of $f_\gamma \sim 5 \times 10^{60} M_\odot^{-1}$ at $z \sim 11$, decreasing at lower redshifts. Since such an evolution is degenerate with a slight change $f_{\rm esc}(z)$, we do not expect this to be important. We used their fit for $\dot{\rho}_*(z)$, which was extrapolated beyond $z \sim 7$ from the observed data (overproducing $\dot{\rho}_*(z = 10)$ according to Oesch et al. 2012), and an evolving escape fraction, $f_{\rm esc}(z) =$

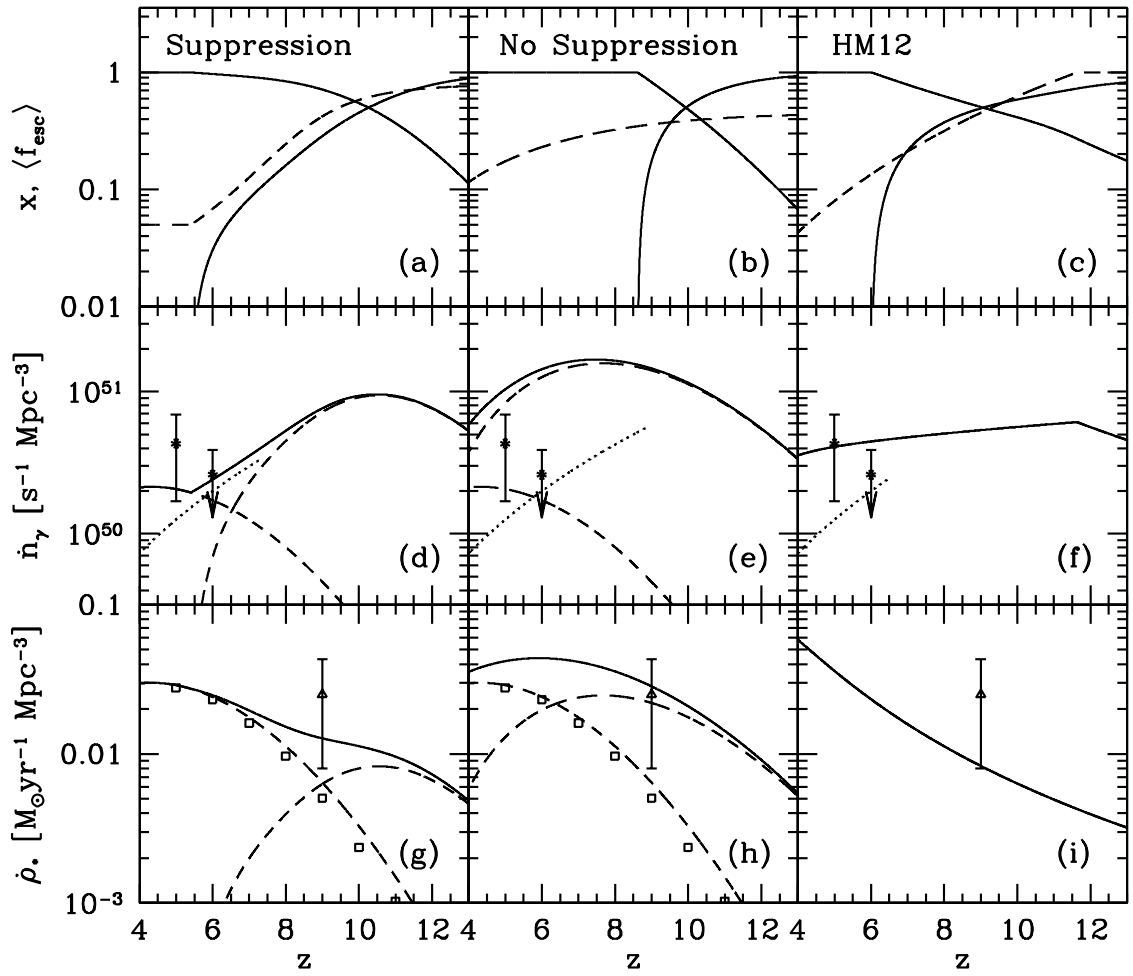

FIG. 1.— *top*: Ionized fraction $x(z)$ and neutral fraction $1-x(z)$. The dashed line shows the mean escape fraction *middle*: Comoving ionizing photon emissivity $\dot{n}_\gamma(z)$ (solid), as well as the contribution from halos in each of our two mass ranges (dashed). Solid points with errorbars show measurements from the Lyman-alpha forest at z =5–6, as compiled by Kuhlen & Faucher-Giguère (2012, see their Table 2 and references therein). Dotted lines indicate the emissivity required to keep the universe ionized, $\dot{n}_\gamma = n_0/\langle t_{\rm rec}\rangle$, and are only plotted for redshifts such that $x > 0.9$. *bottom*: Comoving SFRD, $\dot{\rho}_*(z)$, for each of the models (solid), as well as the contribution from halos in each of our two mass ranges (dashed). The triangular point with errorbars is the value obtained from GRB observations at $z \sim 9$ by Robertson & Ellis (2012). Square points indicate a fit to the observed SFRD for halos with $M > 2\times10^9 M_\odot$, and its extrapolation to $z \geq 8$ (Trenti et al. 2010).

$1.8\times10^{-4}(1+z)^{3.4}$. For the HM12 model, we also obtained $\tau_{\rm es} = 0.086$. In all three cases we used $f_\gamma = 4.5\times10^{60}M_\odot^{-1}$.

3.1. *With suppression*

As seen in panel (a) of Figure 1, the ionized fraction x passes 50% at $z\sim10$ and 90% at ~7. Also shown in panel (a) is the mean emission-weighted escape fraction, defined by

$$\langle f_{\rm esc}\rangle(z) = \frac{\dot{n}_\gamma(z)}{f_\gamma\dot{\rho}_*(z)}. \quad (5)$$

The escape fraction rises from ~0.05 at $z<6$, to ~0.8 at $z=11$. This evolution is entirely due to the evolution in the underlying source population – as the universe becomes more neutral, more ionizing photons come from photosuppressible halos, which have much higher escape fractions.

The ionizing emissivity is shown in panel (d), as well as constraints from table 2 of Kuhlen & Faucher-Giguère (2012), derived by combining measurements of the mean free path (e.g., Songaila & Cowie 2010) with the transmissivity of the Lyman-α forest (e.g., Bolton & Haehnelt 2007). It reaches a peak of $\dot{n}_\gamma \sim 10^{51}{\rm s}^{-1}{\rm Mpc}^{-3}$ at $z\sim11$. The upturn at $z\sim5$ is due to the rise of higher mass sources, in particular from halos above $2\times10^9M_\odot$. The main sources of reionization in this model do not contribute substantially to the emissivity at $z<6$, consistent with *both* an early reionization that satisfies the WMAP optical depth, *and* a photon-starved end to reionization. The star formation rate density rises from $\dot{\rho}_* \sim 10^{-3}M_\odot{\rm yr}^{-1}{\rm Mpc}^{-3}$ at $z=16$, plateaus at ~0.01 over $z\sim8-12$, increasing at $z<12$. (panel g). Shown also are values from the ICLF model of Trenti et al. (2010) integrated down to a minimum halo mass of $2\times10^9M_\odot$ – our model matches the predicted evolution of the SFRD of Lyman-break galaxies. By $z\sim13$, star formation occurring in suppressible halos accounts for over 90 per cent of the total SFRD.

3.2. *No suppression*

As seen in panel (b), overlap occurs earlier in the model without suppression, at $z \sim 8.5$ (as compared to $z \sim 5.5$ in the suppression model). The post-reionization ionizing emissivity is higher without suppression, $\dot{n}_\gamma > 10^{51}\mathrm{s}^{-1}\mathrm{Mpc}^{-3}$ for $z \gtrsim 5$ (panel e). This violates inferences from the Lyman-α forest at $z \sim 5-6$, which indicate values at those redshifts of $\sim 2-4\times10^{50}\mathrm{s}^{-1}\mathrm{Mpc}^{-3}$ (data points in Figure 1; Bolton & Haehnelt 2007; Kuhlen & Faucher-Giguère 2012), and would be difficult to reconcile with the appearance of the Gunn-Peterson trough at $z \gtrsim 6$ (e.g., Fan et al. 2002; Willott 2007). We were unable to find a model with $\epsilon_{*,1} \leq \epsilon_{*,2}$ and $f_{\mathrm{esc},2} \leq 0.05$ that simultaneously satisfies the constraints and does not include suppression.

3.3. *Minimal reionization model of HM12*

In Figure 1, we show results from our implementation of the "minimal reionization model" of HM12. Shown in panel (c) is the escape fraction, $f_{\mathrm{esc}} \propto (1+z)^{3.4}$. Since $\dot{n}_\gamma \propto f_{\mathrm{esc}}\dot{\rho}_*$, the drop in the SFRD towards higher redshift in panel (i) is roughly canceled by the increasing f_{esc}, so that $\dot{n}_\gamma$ is nearly flat (panel f). Notice that scenarios where the ionizing emissivity is flat struggle to reproduce the upper limit to the emissivity at $z = 6$. By contrast, the suppression model naturally accommodates this limit with an increasing contribution from fainter sources at higher redshifts (panel d). However, the upper limit at $z = 6$ ($\dot{n}_\gamma < 2.6\times10^{50}\mathrm{s}^{-1}\mathrm{Mpc}^{-3}$) could be higher, as it is based on combining inferred photoionization rates (Bolton & Haehnelt 2007) with highly-uncertain estimates of the mean free path at $z = 6$ (Songaila & Cowie 2010). A lower mean free path than assumed by Kuhlen & Faucher-Giguère (2012), which was based upon a fit which lies above the $z = 5.7$ data point from Songaila & Cowie (2010), would result in a higher upper limit.

Both the HM12 model and our suppression model exhibit a similarly strong evolution in the mean escape fraction, with f_{esc} of order unity for $z > 10$, and $f_{\mathrm{esc}} \sim 0.05$ at $z \sim 5$. In the suppression model, this is a natural outcome of the assumption that the low-mass halos have high escape fractions and dominate the ionizing photon budget early ($f_{\mathrm{esc},1} = 0.8$), but by the end of reionization only the more massive halos host stars, and the escape fraction is about a factor of 15 lower ($f_{\mathrm{esc},2} = 0.05$). Suppression can therefore be viewed as a physical explanation for the strongly evolving escape fraction needed to satisfy the observational constraints.

Comparing the SFRDs assumed by the HM12 and the suppression model reveals that they agree to within a factor of 2 for all z =5–13. In detail, the SFRD in the HM12 model uses an extrapolation to $z > 8$ of a fitting function constrained at $z < 8$:

$$\dot{\rho}_* = \left[6.9\times10^{-3} + 0.14\frac{(z/2.2)^{1.5}}{1+(z/2.7)^{4.1}}\right] M_\odot\mathrm{yr}^{-1}\mathrm{Mpc}^{-3}. \quad (6)$$

The suppression model predicts that the mass range dominating star formation transitions smoothly from photosuppressible halos to more massive ones around z =8–10. In fact, comparing the dashed curves in panel (g) with the SFRD in panel (i), the HM12 model depends on either the increasing role of sources that cannot be detected in the post-reionization Universe (including photosuppressible halos), or a strongly increasing star formation efficiency in LBGs.

4. DISCUSSION AND OBSERVATIONAL IMPLICATIONS

In this letter we presented a reionization model that can simultaneously satisfy all the current observational constraints on hydrogen reionization (Lyman-α forest at $z \sim 5-6$, SFRD from Lyman-break galaxy surveys at $z \sim 6-10$, low escape fractions at $z \lesssim 6$, and WMAP τ_{es}). Our model predicts that the majority of the ionizing photons at $z \gtrsim 9$ are produced in faint galaxies hosted in photosuppressible dark matter halos with $M \sim 10^{8.5}\ M_\odot$, undetectable in current surveys (Trenti et al. 2010; Muñoz & Loeb 2011; Kuhlen & Faucher-Giguère 2012). Once reionization is completed, the star formation in these halos is suppressed by radiative feedback, so that these sources do not contribute to the ionizing emissivity at lower redshift. Therefore, we predict that the sources of reionization are primarily galaxies with $L < 0.06L_*(z = 3)$, too faint to be detected by even the deepest HST observations.

A key prediction is that the SFRD is higher than that inferred from Lyman-break galaxy surveys, by a factor of ~ 2 at $z = 9$, increasing to a factor of ~ 10 at $z = 12$. Indeed, alternate tracers of star formation indicate that this is likely. Estimates of $\dot{\rho}_*$ from the GRB rate measure $\dot{\rho}_* \sim 0.025^{+0.018}_{-0.017}\ \mathrm{M}_\odot\mathrm{yr}^{-1}\mathrm{Mpc}^{-3}$ at $z \sim 9$ (Robertson & Ellis 2012; see also Kistler et al. 2009), one order of magnitude higher than the LBG surveys estimate. In addition, the non-detection of GRB host galaxies at $z > 5$ in ultradeep HST images provides an independent confirmation that the majority of star formation at those redshifts is happening in galaxies fainter than current observational limits (Trenti et al. 2012). Finally, the latest determination of the galaxy luminosity function at $z \sim 8$ has a very steep faint-end slope ($\alpha = -1.98 \pm 0.2$) at $M_{\mathrm{AB}} \sim -17.7$, implying a logarithmically divergent contribution to the SFRD from fainter, unseen galaxies (Bradley et al. 2012). All these observations are naturally explained in the framework presented here based on photosuppressible halos providing most of the reionizing photons.

It is useful to compare the SFRD and escape fractions we obtain to that of the HM12 model, which is based on the SFRD in galaxies with $L > 0.06L_*$ at $z = 2-7$. In our framework the sources of reionization at $z \sim 10$ will remain unseen in near-future galaxy surveys at $z \sim 10$ – our photosuppressible halos correspond to $-15 \lesssim M_{\mathrm{AB}} \lesssim -10$ over $z \simeq 6-12$. If the SFRD in the HM12 model comes from galaxies of the same UV luminosities as at lower redshifts, their extrapolation to $z = 10$ is likely too high and marginally inconsistent with the strong decline in the LBG population between $z = 8$ and $z = 10$ observed by Oesch et al. (2012, see their Fig. 8).

Even assuming a SFRD due to bright galaxies that is not declining as quickly as suggested by the LBG observations, it is still necessary to assume an escape fraction that is a strongly increasing function of redshift in order to satisfy the WMAP τ_{es} constraint. Such an evolution is naturally explained in our model, where the average escape fraction increases to high redshift simply because there are more low-mass halos forming in the unheated regions.

The high escape fractions for faint galaxies favored in our model should have a unique signature in the cosmic infrared background (Fernandez et al. 2012). This is because the Lyman-α emission per escaping ionizing photon is inversely proportional to the escape fraction. A larger escape fraction for a fixed ionization history will result in a lower overall flux and fluctuation amplitude.

There are several important caveats. First, we have assumed that the star formation efficiency in photosuppress-

ible halos is the same as more massive ones. Simulations by Wise et al. (2012) that include the effects of radiation pressure, supernova feedback, and metal-line cooling, find $\dot{M}_* \sim 2\times10^{-2}M_\odot \mathrm{yr}^{-1}$ for a $2\times10^8 M_\odot$ halo at $z = 8$, implying that ~ 0.03 of the gas accreted after reaching the atomic cooling limit is converted to stars, consistent with our choice of $\epsilon_{*,1} = 0.03$. The simulations of Finlator et al. (2011), on the other hand, exhibit a much lower star formation rate at a similar mass of a few times $10^8 M_\odot$. Although theoretical predictions have not converged, $\epsilon_{*,1} \simeq \epsilon_{*,2}$ seems plausible.

In addition, we have assumed that the suppression operates instantaneously within H II regions. Although this is an oversimplification, it illustrates the basic trends resulting from high escape fractions and suppression in low-mass halos. Detailed numerical simulations that self-consistently include both external and internal radiative feedback during reionization will be required to address these issues more accurately.

Finally, we note that the best-fitting value for the electron scattering optical depth from WMAP, $\tau_{\rm es} = 0.088$, has 1-σ error bars of of ~ 0.015, indicating that the true value could be as low as $\tau_{\rm es} \sim 0.06$, at 2-σ. In our model with suppression, $\tau \sim 0.06$ can be achieved with a lower escape fraction for low mass halos, $f_{\rm esc,1} \sim 0.2$. This is still however a factor of four times higher than that for the larger mass halos, $f_{\rm esc} = 0.05$. Upcoming measurements with the Planck satellite will be essential in tightening constraints on $\tau_{\rm es}$ and therefore on the nature of the first galaxies.

We thank T. Abel and R. Wechsler for helpful discussions, M. McQuinn and S. P. Oh for comments on an earlier draft, the anonymous referee, and the Kavli Institute for Theoretical Physics, Santa Barbara, for their hospitality during the workshop “First Galaxies and Faint Dwarfs: Clues to the Small Scale Structure of Cold Dark Matter", where this work was initiated. This research was supported in part by the National Science Foundation under Grant No. NSF PHY11-25915.

REFERENCES

Ahn, K., Iliev, I. T., Shapiro, P. R., Mellema, G., Koda, J., & Mao, Y. 2012, ArXiv e-prints
Bolton, J. S. & Haehnelt, M. G. 2007, MNRAS, 382, 325
Bouwens, R. J., Illingworth, G. D., Oesch, P. A., Trenti, M., Labbe, I., Franx, M., Stiavelli, M., Carollo, C. M., van Dokkum, P., & Magee, D. 2011, ArXiv e-prints
Bradley, L. D., Trenti, M., Oesch, P. A., Stiavelli, M., Treu, T., Bouwens, R. J., Shull, J. M., Holwerda, B. W., & Pirzkal, N. 2012, ArXiv e-prints
Cen, R. 2003, ApJ, 591, 12
Choudhury, T. R. & Ferrara, A. 2006, MNRAS, 371, L55
Dijkstra, M., Haiman, Z., Rees, M. J., & Weinberg, D. H. 2004, ApJ, 601, 666
Efstathiou, G. 1992, MNRAS, 256, 43P
Fan, X., Carilli, C. L., & Keating, B. 2006, ARA&A, 44, 415
Fan, X., Narayanan, V. K., Strauss, M. A., White, R. L., Becker, R. H., Pentericci, L., & Rix, H.-W. 2002, AJ, 123, 1247
Fernandez, E. R., Dole, H., & Iliev, I. T. 2012, ArXiv e-prints
Finlator, K., Davé, R., & Özel, F. 2011, ApJ, 743, 169
Fontanot, F., Cristiani, S., & Vanzella, E. 2012, ArXiv e-prints
Gnedin, N. Y. 2000, ApJ, 542, 535
Gnedin, N. Y. & Hui, L. 1998, MNRAS, 296, 44
Gnedin, N. Y., Kravtsov, A. V., & Chen, H.-W. 2008, ApJ, 672, 765
Gunn, J. E. & Peterson, B. A. 1965, ApJ, 142, 1633
Haardt, F. & Madau, P. 2012, ApJ, 746, 125
Haiman, Z. & Bryan, G. L. 2006, ApJ, 650, 7
Haiman, Z. & Holder, G. P. 2003, ApJ, 595, 1
Iliev, I. T., Mellema, G., Shapiro, P. R., & Pen, U.-L. 2007, MNRAS, 376, 534
Iwata, I., Inoue, A. K., Matsuda, Y., Furusawa, H., Hayashino, T., Kousai, K., Akiyama, M., Yamada, T., Burgarella, D., & Deharveng, J.-M. 2009, ApJ, 692, 1287
Kistler, M. D., Yüksel, H., Beacom, J. F., Hopkins, A. M., & Wyithe, J. S. B. 2009, ApJ, 705, L104
Komatsu, E., Smith, K. M., Dunkley, J., Bennett, C. L., & et al. 2011, ApJS, 192, 18
Kuhlen, M. & Faucher-Giguère, C.-A. 2012, MNRAS, 2875
Muñoz, J. A. & Loeb, A. 2011, ApJ, 729, 99
Nestor, D. B., Shapley, A. E., Steidel, C. C., & Siana, B. 2011, ApJ, 736, 18
Oesch, P. A., Bouwens, R. J., Illingworth, G. D., Labbé, I., Trenti, M., Gonzalez, V., Carollo, C. M., Franx, M., van Dokkum, P. G., & Magee, D. 2012, ApJ, 745, 110
Okamoto, T., Gao, L., & Theuns, T. 2008, MNRAS, 390, 920
Pawlik, A. H., Schaye, J., & van Scherpenzeel, E. 2009, MNRAS, 394, 1812
Razoumov, A. O. & Sommer-Larsen, J. 2010, ApJ, 710, 1239
Ricotti, M. & Ostriker, J. P. 2004, MNRAS, 352, 547
Robertson, B. E. & Ellis, R. S. 2012, ApJ, 744, 95
Schaerer, D. 2002, A&A, 382, 28
Shapiro, P. R. & Giroux, M. L. 1987, ApJ, 321, L107
Shapiro, P. R., Giroux, M. L., & Babul, A. 1994, ApJ, 427, 25
Shapley, A. E., Steidel, C. C., Pettini, M., Adelberger, K. L., & Erb, D. K. 2006, ApJ, 651, 688
Shull, J. M., Harness, A., Trenti, M., & Smith, B. D. 2012, ApJ, 747, 100
Siana, B., Teplitz, H. I., Ferguson, H. C., Brown, T. M., Giavalisco, M., Dickinson, M., Chary, R.-R., de Mello, D. F., Conselice, C. J., Bridge, C. R., Gardner, J. P., Colbert, J. W., & Scarlata, C. 2010, ApJ, 723, 241
Songaila, A. & Cowie, L. L. 2010, ApJ, 721, 1448
Thoul, A. A. & Weinberg, D. H. 1996, ApJ, 465, 608
Trenti, M., Perna, R., Levesque, E. M., Shull, J. M., & Stocke, J. T. 2012, ApJ, 749, L38
Trenti, M., Stiavelli, M., Bouwens, R. J., Oesch, P., Shull, J. M., Illingworth, G. D., Bradley, L. D., & Carollo, C. M. 2010, ApJ, 714, L202
Willott, C. J. e. a. 2007, AJ, 134, 2435
Wise, J. H., Abel, T., Turk, M. J., Norman, M. L., & Smith, B. D. 2012, arXiv:1206.1043
Wise, J. H. & Cen, R. 2009, ApJ, 693, 984
Wyithe, J. S. B. & Loeb, A. 2003, ApJ, 588, L69